Available online at www.sciencedirect.com
ScienceDirect
Coordination Chemistry Reviews 251 (2007) 2606–2621
COORDINATION CHEMISTRY REVIEWS
www.elsevier.com/locate/ccr

Review

Spin crossover iron(III) complexes

Masayuki Nihei [a], Takuya Shiga [a], Yonezo Maeda [b], Hiroki Oshio [a,*]

[a] *Graduate School of Pure and Applied Sciences, University of Tsukuba, Tennodai 1-1-1, Tsukuba 305-8571, Japan*
[b] *Department of Chemistry, Kyushu University, Hakozaki 6-10-1, Higashi-ku, Fukuoka 812-8581, Japan*

Received 30 January 2007; accepted 7 August 2007
Available online 11 August 2007

Contents

Abstract

Metal complexes, of which metal ions have d^4–d^7 electrons, may exhibit spin conversion by external stimuli, and they are called spin crossover (SCO) complexes. SCO complexes are classified into two groups depending on spin transition behavior—(i) spin transition (ST) type: the spin transition between high-spin (HS) and low-spin (LS) states occurs abruptly or discontinuously within a few Kelvin. (ii) Spin equilibrium (SE) type: the spin transition occurs gradually over a wide temperature range. Note that spin transitions in some SE type SCO complexes occur very rapidly and their transition rate is the order of 10^7 s^{-1}. In this article, X-ray structural and magnetic studies on ferric SCO complexes are presented and the possible origin of the rapid spin interconversion is discussed.

Keywords: Spin crossover; Iron; Magnetism; Mössbauer spectrum; Relaxation

1. Introduction

Since the discovery of an anomalous magnetic behavior, called spin crossover (SCO), in tris(*N*,*N*-dialkyldithio-

* Corresponding author. Tel.: +81 29 853 4238; fax: +81 29 853 4238.
E-mail address: oshio@chem.tsukuba.ac.jp (H. Oshio).

0010-8545/$ – see front matter © 2007 Elsevier B.V. All rights reserved.
doi:10.1016/j.ccr.2007.08.007

carbamato)iron(III) complexes [1], the spin crossover phenomena in iron(II) [2] and iron(III) [3] complexes have been extensively studied [4]. SCO complexes are classified into two groups as stated in the abstract, and their spin transition behavior depends upon intramolecular Jahn–Teller distortions [5] and intermolecular interactions [6]. Heat capacity measurements for SCO systems revealed that the total entropy changes (ΔS) accompanied with spin transitions are much larger than the values expected for the spin conversions between the LS and HS states: $\Delta S = 9.13$ ($=R \ln 3$) and 13.38 ($=R \ln 5$) J K^{-1} mol^{-1} for iron(III) and iron(II) systems, respectively. The extra entropy changes are due to phonon systems and order–disorder phenomena. The different spin transition behavior can be explained by theoretical models, such as the domain model, regular solution model and elastic phonon model [7], and herein we address the first model. The domain size (a number of molecules in the domain) for ST types (95 for $[Fe(phen)_2(NCS)_2]$) is larger than that for SE types (5 for $[Fe^{III}(acpa)_2]PF_6$). This suggests that the spin transitions in ST type complexes couple strongly with the lattice phonon system. It is noted that some SE complexes interconvert their spin states faster than the reciprocal of the ^{57}Fe Mössbauer lifetime (10^{-7} s). The fast spin interconversion phenomena have been recognized in iron(III) SCO complexes [8–12]. In this article, iron(III) SCO systems are reviewed.

2. Spin crossover iron(III) complexes

Structures and SCO behavior of iron(III) complexes are presented in this section, and more detailed discussions can be also found in another review [13].

2.1. Spin crossover iron(III) complexes with chalcogen donor atoms

SCO phenomena were first discovered in the tris(*N,N*-dialkyldithiocarbamato)iron(III) compounds [14]. Dithiocarbamate acts as a bidentate ligand with two donating sulfur atoms and an iron ion has an FeS_6 chromophore. Since the discovery of the first iron(III) SCO complexes, the SCO behavior of its derivatives has been investigated by means of various physical measurements [15]. Most SCO complexes with dithiocarbamate show gradual spin transitions, classified into the SE type. SCO behavior of iron(III) dithiocarbamates in solution are similar to that in solid. Enthalpy variations (ΔH) accompanied with the spin transitions are in the range of 500–750 cm^{-1}, suggesting that the domain size (the number of molecules showing cooperativity) is close to unity [16]. SCO behaviors in these complexes strongly depend on the substituents of dithiocarbamato ligands, because steric intramolecular interactions cause different coordination geometries. Coordination geometry of an FeS_6 core has a pseudo-D_3 symmetry, which is intermediate between octahedral and trigonal prismatic stereochemistry. The average Fe–S bond length is about 2.4 Å in the HS state, which is longer than that in the LS state. Mössbauer spectra of dithiocarbamate systems exhibited a broad single quadrupole doublet at the spin transition temperature, suggesting rapid spin-state interconversion between the two spin states comparable to the ^{57}Fe Mössbauer time scale (>10^7 s^{-1}).

SCO complexes with bidentate chalcogen ligands such as 1,3-disubstituted-monothio-β-diketonate are SE types [10,17]. Complexes have distorted octahedral FeO_3S_3 geometry and exhibit gradual SCO behavior, except for the methyl substituted system with a relatively abrupt spin interconversion at $T_{1/2}$ = ca. 150 K ($T_{1/2}$: temperature with 1:1 ratio of HS and LS species both for the first and second order phase transitions).

2.2. Spin crossover iron(III) complexes with multidentate Schiff-base type ligands

Iron(III) complexes with multidentate Schiff bases are one of the most established iron(III) SCO systems and their SCO behavior can be tuned by chemical modification of ligands. Schiff-base ligands in iron(III) SCO complexes are classified into four groups: (1) asymmetric and (2) symmetric Schiff bases derived from salicylaldehyde, and (3) asymmetric and (4) symmetric Schiff bases derived from acetylacetone. Scheme 1 summarizes multidentate Schiff-base ligands, often used in SCO iron(III) complexes.

2.2.1. Complexes with asymmetrical Schiff bases derived from salicylaldehyde

Condensation reactions of salicylaldehyde with amine derivatives afford various tridentate Schiff-base ligands. Some SCO iron(III) complexes with tridentate Schiff bases, $[Fe(L)_2]X$ (L = mono-anionic Schiff-base derivatives with a N_2O chromophore, and X = counter anions), are shown in Fig. 1.

SCO behavior in $[Fe(qsal)_2]X{\cdot}solv$ (X = Cl, Br, I, NCS, NCSe) (Fig. 1a) [18] and $[Fe(pap)_2]X{\cdot}solv$ (X = NO_3, BPh_4, PF_6, ClO_4, NCS) are strongly dependent on counter anions and/or solvent molecules. $[Fe(qsal)_2]Cl{\cdot}2H_2O$ shows incomplete SCO, while $[Fe(qsal)_2]Br{\cdot}H_2O$ and $[Fe(qsal)_2]I$ are HS and LS complexes, respectively [19]. $[Fe(qsal)_2]NCS$ shows intriguing SCO behavior depending on synthetic conditions [8e]. $[Fe(qsal)_2]NCS$ prepared from methanolic solution at 298 K shows a large hysteresis loop (width of 70 K) accompanied with spin transitions. In the heating process, two-step changes in magnetic moment occurred at 220 and 270 K, which might be due to the existence of two phases or isomers with different transition temperatures. When $[Fe(qsal)_2]NCS$ is prepared from methanol below 280 K, the complex is predominantly in the LS state and the magnetic behavior was changed by aging. After standing for 10 days, the complex showed SCO with a hysteresis loop (width of 70 K) centered at 286 K. SCO behavior in $[Fe(pap)_2]X{\cdot}solv$ (X = NO_3, BPh_4, PF_6, ClO_4, NCS) is also significantly affected by counter anions and solvent molecules [8e]. Solvent free NO_3^- and BPh_4^- salts are HS, whereas the PF_6^- salt is LS. Freshly prepared $[Fe(pap)_2]ClO_4$ exhibits SCO with hysteresis at $T_{1/2}\uparrow = 262$ K and $T_{1/2}\downarrow = 242$ K ($T_{1/2}\uparrow$ and $T_{1/2}\downarrow$ represent transition temperatures in heating and cooling processes, respectively), respectively [20]. The transition temperature shifted to 150 K after storage for one week. Elemental analyses and powder X-ray diffraction data suggested

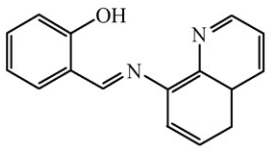

Hqsal

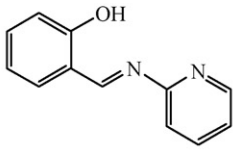

Hpap

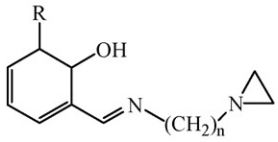

HsalAEA : n = 2, R = H
HsalAPA : n = 3, R = H
H3-OEt-salAPA : n = 3, R = OEt

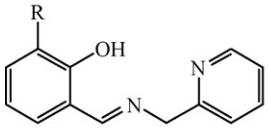

Hsapa : R = H
Hvapa : R = OMe

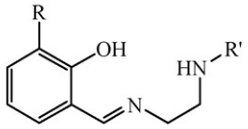

HsalEen : R = H, R' = Et
H3-OMe-salEen : R = OMe, R' = Et
H3-R-salBzen : R = OEt or allyl, R'=benzyl

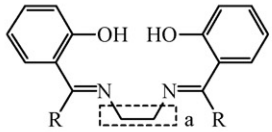

H_2salen : R = H, a= CH_2CH_2
H_2hapten : R = Me, a= CH_2CH_2
H_2salphen : R = H, a= C_6H_4
H_2sal$_2$trien : R = H, a= $(CH_2)_2NH(CH_2)_2NH(CH_2)_2$

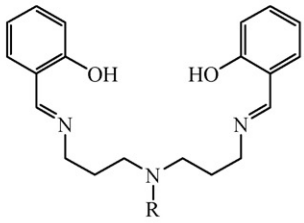

H_2salten : R = H

H_2sal$_2$3, 3, 3 - tet : n = 3
H_2sal$_2$3, 3, 3 - tet : n = 2

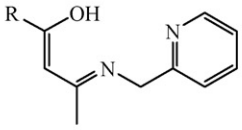

Hacpa : R = Me
Hbzpa : R = Ph

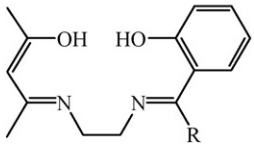

H_2salacen : R = H
H_2hapacen : R = Me

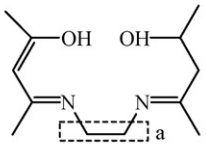

H_2acen : a = CH_2CH_2
H_2acac$_2$trien : a = $(CH_2)_2NH(CH_2)_2NH(CH_2)_2$

Scheme 1.

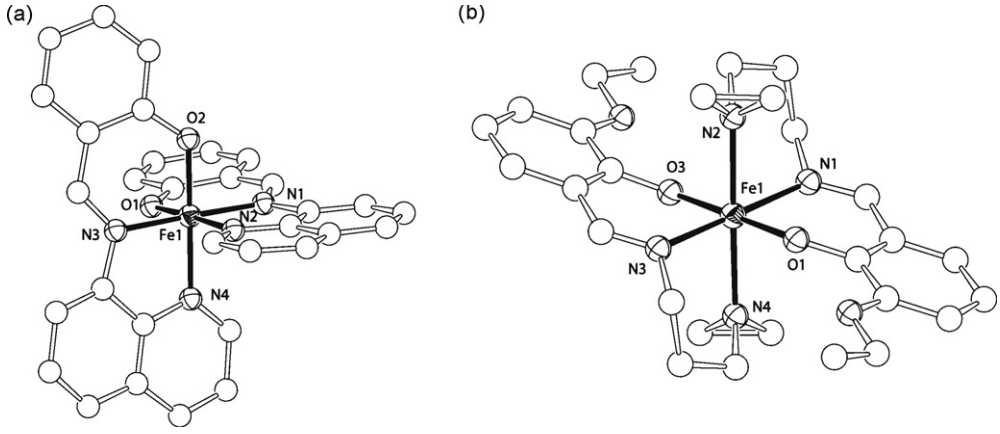

Fig. 1. Structures of the cation in (a) [Fe(qsal)$_2$]NCSe and (b) [Fe(3-OEt-salAPA)$_2$]$ClO_4 \cdot C_6H_5Cl$ [18,24].

that slight structural changes are responsible for the different SCO behavior. $[Fe(pap)_2]ClO_4 \cdot H_2O$ and $[Fe(pap)_2]PF_6 \cdot MeOH$ exhibit abrupt spin transitions with hysteresis ($T_{1/2}\uparrow = 180$ K and $T_{1/2}\downarrow = 165$ K) and $T_{1/2} = 288$ K without hysteresis, respectively [21,22].

A series of $[Fe(3\text{-OEt-salAPA})_2]ClO_4 \cdot n(solv)$ classified into the SE type have been systematically studied. $[Fe(3\text{-OEt-salAPA})_2]ClO_4 \cdot nCH_2Cl_2$ showed gradual SCO at $T_{1/2} = 295$ K ($n = 0$) and $T_{1/2} = 152$ K ($n = 1$) [23]. X-ray crystallographic analyses for $[Fe(3\text{-OEt-salAPA})_2]ClO_4 \cdot C_6H_5X$ (Fig. 1b) at various temperatures showed that $Fe–N_{amine}$ bonds are longer than Fe–O bonds [3c,8a,24]. The octahedral coordination become more distorted upon SCO, and the changes in coordination bond lengths are most significant in $Fe–N_{amine}$ bonds. Coordinating 3-OEt-salAEA$^-$ has a five-membered chelate ring, which is in contrast to six-membered ones in 3-OEt-salAPA$^-$. $[Fe(3\text{-OEt-salAEA})_2]ClO_4$ is predominantly in the HS state even at 20 K [25]. Iron(III) complexes with tridentate ligands of sapa$^-$ (six-membered chelate ring) and vapa$^-$ (five membered one) are HS or SCO complexes [8f]. It is expected that chelate ligands with five membered rings give stronger ligand field than that with six-membered rings.

Counter anions affect SCO behavior. $[Fe(salEen)_2]BPh_4 \cdot 0.5H_2O$ and $[Fe(3\text{-OMe-salEen})_2]BPh_4$ are HS, and $[Fe(3\text{-OMe-salEen})_2]NO_3 \cdot 0.5H_2O$ are predominantly LS, while PF_6^- salts showed SCO behavior [26]. $[Fe(salEen)_2]PF_6$ undergoes a gradual SCO at $T_{1/2} = 159$ K [26b]. A SCO behavior in $[Fe(3\text{-OMe-salEen})_2]PF_6$ is, in contrast, very abrupt with thermal hysteresis (width of 2–4 K) [26]. The iron(III) complexes with salBzen$^-$ are HS species for Cl^- and NO_3^- salts, $[Fe(3\text{-OMe-salBzen})_2]BPh_4 \cdot CH_3CN$ is, on the other hand, a SE type SCO complex [27]. The SCO behavior is strongly affected by sample treatments. Grinding samples leads to the gradual and incomplete spin transition, which is due to defects and stress generated in the samples.

2.2.2. *Complexes with symmetrical Schiff bases derived from salicylaldehyde*

Symmetrical quadridentate Schiff-base ligands are obtained by condensation reactions of salicylaldehyde with diamino derivatives. H_2salen and H_2salphen are the most commonly used quadridentate ligands with an N_2O_2-donor set. Reactions of ligands with iron(III) and NO^- ions yield five coordinated iron(III) complexes with FeN_3O_2 core [28]. This class of complexes exhibits characteristic SCO between LS ($S = 1/2$) and intermediate spin (IS: $S = 3/2$) states. [Fe(salen)NO] shows an abrupt $S = 1/2 \leftrightarrow S = 3/2$ spin transition associated with a hysteresis loop centered at 175 K [28a]. Although [Fe(salen)NO] showed no crystallographic phase transition upon spin transition from IS to LS states relatively large changes in coordination bond lengths were observed (Fig. 2a) [29]. The average bond lengths of Fe–N bond are 2.075 Å at 296 K and 1.974 Å at 98 K, respectively. [Fe(salphen)NO] showed gradual spin transition from IS to LS states [30] which is in contrast to [Fe(salen)NO]. ^{57}Fe Mössbauer spectra revealed that the spin interconversion in [Fe(salphen)NO] occurs faster than Mössbauer time scale, while the interconversion in [Fe(salen)NO] is slow.

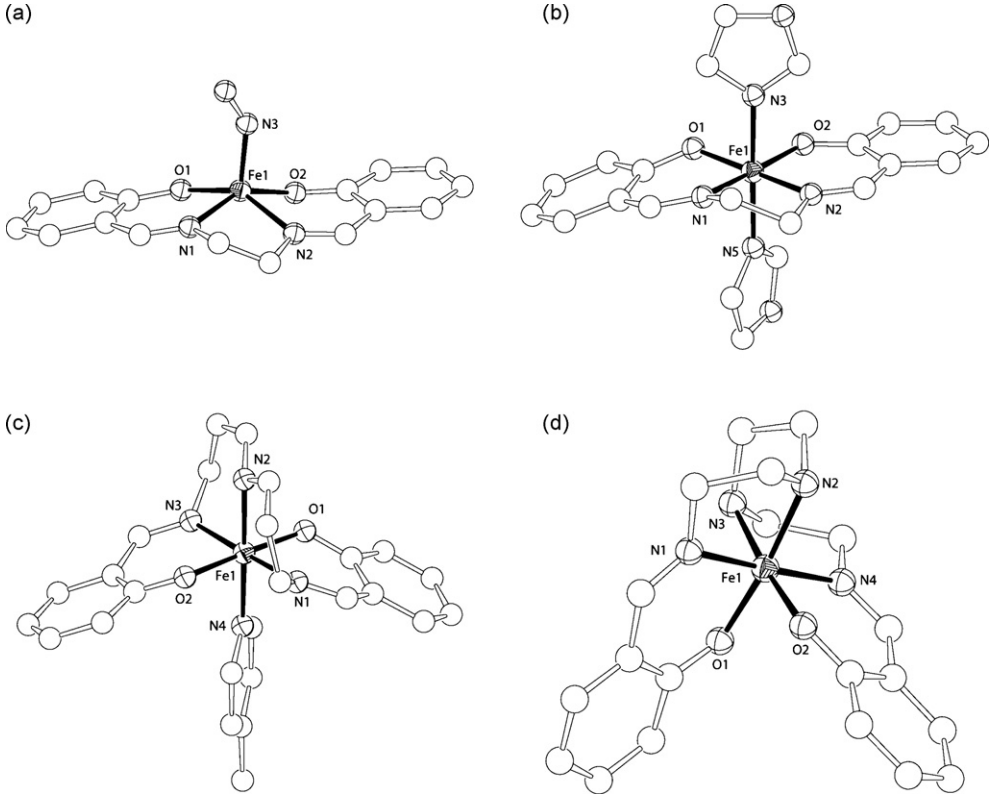

Fig. 2. Structure of (a) [Fe(salen)NO], and structures of the cations in (b) $[Fe(salen)(Him)_2]ClO_4$, (c) [Fe(salten)(4-methylpyridine)]BPh_4, and (d) $[Fe(sal_2trien)]Br \cdot 2H_2O$ [29,31a,32,34].

A variety of six-coordinated iron(III) complexes with FeN_4O_2 chromophore was prepared by using quadridentate Schiff-base ligands with N_2O_2 donor atoms and monodentate heterocyclic co-ligands. [Fe(salen)(Him)$_2$]X (Him = imidazole and X = PF_6 and BPh_4) are purely HS species, while ClO_4^- and BF_4^- salts show gradual SE [8c,31]. Structures of [Fe(salen)(Him)$_2$]ClO_4 in HS (295 K) and LS (120 K) states were determined (Fig. 2b) [31a]. Subtle changes in Fe–O bond lengths (ΔFe–O_{av}: 0.002 Å) are observed upon SCO, while significant bond length changes of Fe–N bonds are observed (ΔFe–N_{salen}: 0.154 Å and ΔFe–N_{Him}: 0.154 Å). Coordination spheres in [Fe(salen)(Him)$_2$]X depend strongly on spin states and different conformations of chelate ring involving an ethylene backbone of $salen^{2-}$ were observed [31a]. The SCO complexes of ClO_4^- and BF_4^- salts possess an *envelope* configuration about the central iron(III) ions, while the HS PF_6^- salt has a *meso* configuration.

Most iron(III) SCO complexes with quinquedentate ligands have an octahedral FeN_4O_2 coordination with $salten^{2-}$ and heterocyclic N-donating ligands. [Fe(salten)Cl]·CH_3OH and [Fe(salten)CN]·1.5CH_3OH are HS and LS iron(III) complexes, respectively [32]. [Fe(salten)L]BPh_4 (L = pyridine, 3-methyl-pyridine, 4-methyl-pyridine, 3,4-dimethyl-pyridine, and 2-methyl-imidazole) exhibit gradual SCO both in solid and solution associated with color change from dark violet at higher temperature to blue-green at lower temperature [32,33]. An iron(III) ion in [Fe(salten)(4-methyl-pyridine)]BPh4 (Fig. 2c) [32] has a pseudo-octahedral coordination geometry. The equatorial sites are occupied by two imino nitrogen (Fe–Nav = 1.987 Å) and phenoxo oxygen (Fe–O_{av} = 1.885 Å) atoms, while amino nitrogen atoms from $salten2^-$ and nitrogen atoms from 4-methyl-pyridine coordinate from the axial direction with coordination bond lengths of 2.035(7) Å and 2.010(6) Å, respectively.

A symmetric Schiff base of H_2sal_2trien is derived from salicylaldehyde and triethylenetetramine, and acts as a hexadentate N_4O_2 donor (Fig. 2d) [34]. [Fe(sal_2trien)]PF_6 and [Fe(sal_2trien)]BPh_4 show gradual SCO behavior both in solid and solution [34]. Magnetic properties of [Fe(sal_2trien)]X·nH_2O (X = Cl, Br, I, NO_3, PF_6, and BPh_4) are strongly affected by hydration, where a higher degree of hydration, such as complexes with $n = 2$ and X = Cl and Br, leads to the stabilizations of the LS states [34,35]. The differences in the average coordination bond lengths between HS and LS states are ΔFe–O_{av} = 0.04 Å and ΔFe–N_{av} = 0.17 Å for [Fe(sal_2trien)]X·2H_2O. Spin interconversion rates are affected by the number of solvent molecules in the crystals. ^{57}Fe Mössbauer spectra for [Fe(sal_2trien)]BPh_4·*n*(acetone) (*n* = 0 or 1) revealed that solvated compounds exhibit faster spin interconversion than the Mössbauer time scale, while the interconversion in non-solvated complexes are slower [36].

2.2.3. *Complexes with asymmetrical Schiff bases derived from acetylacetone*

Tridentate asymmetric Schiff bases derived from acetyl acetone afford the second family of SCO iron(III) systems. The central iron(III) ion in this series has a distorted octahedral coordination sphere (N_4O_2) with shorter Fe–O bonds than Fe–N bonds. [Fe(acpa)$_2$]X (X = PF_6, and BPh_4) (Fig. 3a), classified as SE type, show gradual and complete spin transitions associated with structural changes [3e,37]. Fe–N bond lengths in [Fe(acpa)$_2$]PF_6 are 1.941(2)–1.989(2) Å at 120 K and 2.081(2)–2.153(2) Å at 298 K, characteristic of LS and HS iron(III) species, respectively. [Fe(acpa)$_2$]BPh_4 shows similar structural and magnetic changes to the PF_6^- salt, the transition temperature is, however, higher than that for BPh_4^- salts. Similar SCO behavior is observed in [Fe(bzpa)$_2$]X (X = ClO_4, and PF_6) [8f,38]. Note that both [Fe(acpa)$_2$]X and [Fe(bzpa)$_2$]X in acetone exhibit reversible thermochromism accompanied with the spin transition [8f].

H_2salacen is an asymmetric quadridentate ligand containing an acetylidenimine moiety. [Fe(salacen)(Him)$_2$]PF_6 (Fig. 3b) [39] and [Fe(salacen)(N-imidazole)$_2$]PF_6 have FeN_4O_2 chromophores with quadridentate $salacen^{2-}$ and they are classified into SE type with gradual and incomplete SCO [39]. The spin interconversion in these SCO complexes also occurs in organic solvents at 200–300 K and thermochromism was observed from green at 200 K to purple at 300 K.

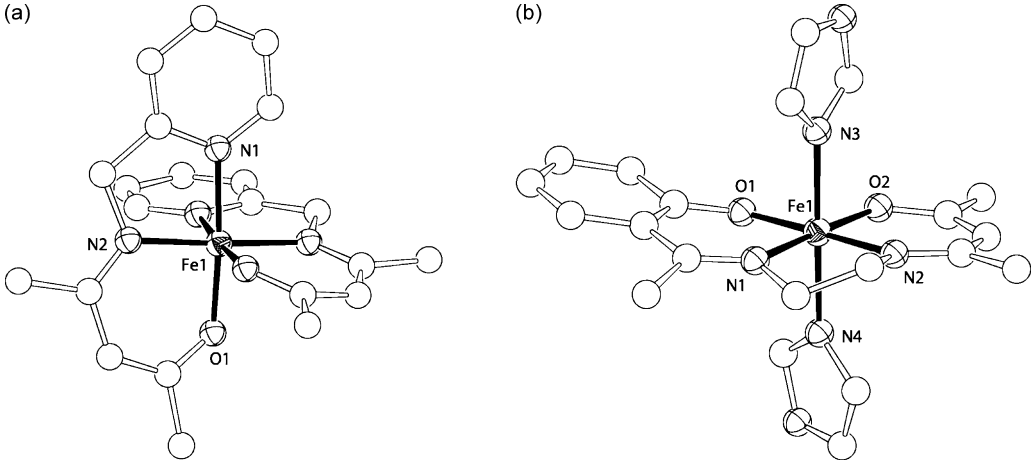

Fig. 3. Structures of the cations in (a) [Fe(acpa)$_2$]PF_6 and (b) [Fe(salacen)(Him)$_2$]PF_6 [37,39].

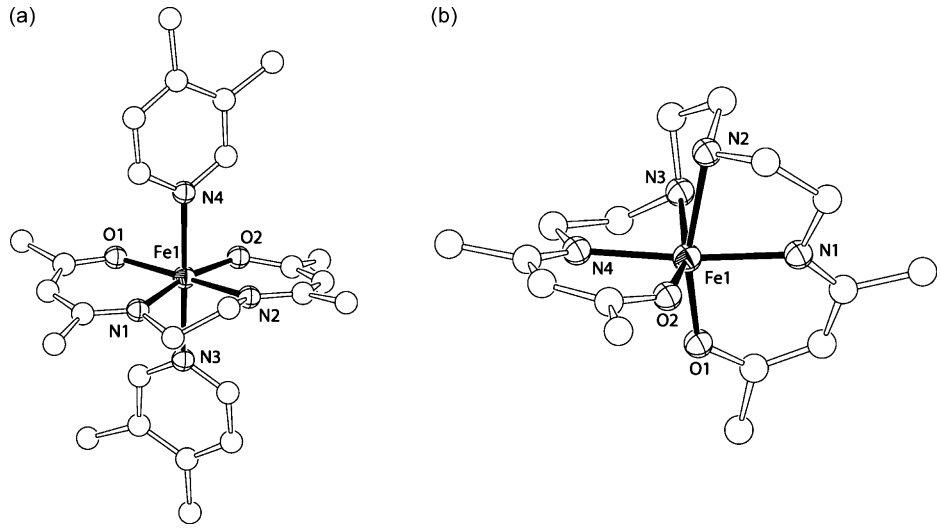

Fig. 4. Structures of the cations in (a) $[Fe(acen)(dmpy)_2]BPh_4$, and (b) $[Fe(acac_2trien)]PF_6$ [8d,41].

2.2.4. Complexes with symmetrical Schiff bases derived from acetylacetone

Reaction of iron sources with symmetrical quadridentate ligands (H_2acen) gave six-coordinated FeN_4O_2 SCO complexes. $[Fe(acen)(dmpy)_2]BPh_4$ (dmpy = 3,4-dimethylpiridine) (Fig. 4a) is an SE type iron(III) SCO complex [8d]. In $[Fe(acen)(dmpy)_2]BPh_4$ the average $Fe–N_{dmpy}$ bond lengths are changed from 1.918 Å to 2.058 Å for $Fe–N_{acen}$ and 2.036 Å to 2.186 Å for $Fe–N_{dmpy}$ upon spin interconversion, while Fe–O bond lengths are not greatly altered [40]. Note that SCO behavior of $[Fe(acen)(dmpy)_2]^+$ is affected by replacements of dmpy with other N-donating heterocyclic co-ligands such as Him, 4-aminoyridine, β-picoline, or γ-picoline [8d,31].

Gradual SCO behavior was observed in a series of $[Fe(acac_2trien)]X$ ($acac_2trien^{2-}$ = hexadentate ligand, and X = Br, I, PF_6, and BPh_4) [35,41], where iron(III) ions have an N_4O_2 chromophore (Fig. 4b). The central iron(III) ion has distorted octahedral coordination geometry with two six-membered and three five-membered chelate rings. Two oxygen atoms of the hexadentate ligand occupy *cis* position and the remaining coordination sites are occupied by two amino and two imino nitrogen atoms in *cis* and *trans* fashions, respectively. All compounds in this family show SCO behavior only in solution except for the BPh_4^- salt, which undergoes SCO also in the solid state [35,41]. $[Fe(acac_2trien)]X$ (X = Br, I, PF_6, and BPh_4) in acetone show thermochromism from red at room temperature to blue at 193 K [42].

2.3. Spin crossover iron(III) complexes with catecholate derivatives

Iron(III) catecholato complexes have been extensively studied as efficient models of catechol dioxygenases [43]. Boillot et al. firstly reported a two-step SCO between LS ($S = 1/2$) and HS ($S = 5/2$) states in $[Fe(cat)(tpa)]BPh_4$ (cat^{2-} = catecholate, tpa = tris(2-pyridylmethyl)amine) (Fig. 5) [44]. Various analogues of $[Fe(R\text{-}cat)(tpa)]X{\cdot}n(solv)$ (R = H, CH_3, OMe, Cl_4, and NO_2 and X = BPh_4, NO_3, PF_6, and ClO_4,) have since been synthesized and shown to be SCO systems [45]. They have distorted octahedral N_4O_2 coordination geometries with quadridentate tpa and catecholate, and their coordination structures changed as temperature was varied. The coordination bond lengths were in the range of 2.03–2.07 Å at 293 K and of 1.93–1.96 Å at 100 K, suggesting the occurrence of SCO. Magnetic susceptibility measurements revealed that most complexes showed gradual SCO, while $[Fe(cat)(tpa)]BPh_4$ showed a relatively abrupt two-step SCO behavior. No significant intermolecular interactions were observed in the crystals, resulting in weak cooperativity, hence, the gradual SCO behavior. Interestingly, $T_{1/2}$ of the complexes vary from 84 K to 253 K depending upon the substituents in catecholates. A linear correlation between $T_{1/2}$ and V/Z (unit cell volume per SCO molecule) was observed, and the difference in $T_{1/2}$ values was ascribed to the chemical pressure effects in the crystals. The detailed mechanism about

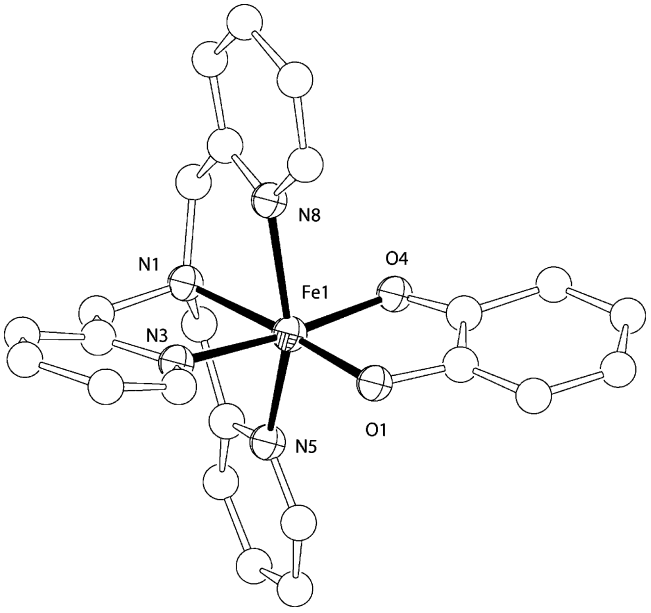

Fig. 5. Structure of the cation in $[Fe(cat)(tpa)_2]BPh_4$ [44b].

two-step SCO in [Fe(cat)(tpa)]BPh_4 was studied by means of X-ray crystal structure analyses and Mössbauer spectroscopy. In [Fe(cat)(tpa)]BPh_4, the complex cations occupy two non-equivalent crystalline sites. Structure analyses revealed that each iron ion is in HS and LS state at 110 K and both cations are in HS states at 220 K, suggesting the occurrence of the subsequent SCO.

2.4. Spin crossover iron(III) complexes with porphyrin derivatives

Iron(III) porphyrins $[Fe^{III}(porphyrin)L_2]^+$ with different spin states have been attracting much interest due to their relevance to catalytic oxidation reactions of cytochrome P450 [46]. Control of spin state in ferric ions can be achieved by chemical modifications of porphyrins and axial ligands, and some complexes showed SCO between HS ($S = 5/2$) and LS ($S = 1/2$) states [47]. On the other hand, a pure IS ($S = 3/2$) is unstable due to the spin–orbit coupling between HS and IS states, which affords a quantum mechanical spin admixture of $S = 5/2$ and 3/2 states. Recently, Nakamura et al. reported quite rare examples of SCO between IS and LS states in iron(III) porphyrins [48]. They studied the spin states of saddle-shaped iron(III) porphyrins with weak axial ligands, $[Fe^{III}(oetpp)L_2]^+$ (oetpp = octaethyltetraphenylporphyrin and L = imidazole (HIm), 4-dimethylaminopyridine (dmap), pyridine (py), 4-cyanopyridine (4-CNpy), and tetrahydrofuran (thf)). The complexes with HIm and dmap are LS complexes, while that with thf is in the IS state. $[Fe^{III}(oetpp)L_2]^+$ (L = py and 4-CNpy) exhibited SCO between IS and LS states, which were characterized by Mössbauer spectra and magnetic susceptibility measurements. Mössbauer spectra of $[Fe^{III}(oetpp)(4\text{-}CNpy)_2]^+$ showed an IS doublet ($\delta = 0.37$ mm s^{-1}, $\Delta E_Q = 3.26$ mm s^{-1}) at 290 K and a new doublet ($\delta = 0.20$ mm s^{-1}, $\Delta E_Q = 2.70$ mm s^{-1}) corresponding to a LS ferric ion appeared at 80 K, suggesting the occurrence of SCO between IS and LS states. $[Fe^{III}(oetpp)(py)_2]^+$ gave one doublet, of which isomer shifts and quadrupole splittings showed a significant temperature dependence between 290 and 90 K. Variable temperature Mössbauer spectra of $[Fe^{III}(oetpp)(py)_2]^+$ revealed the fast SCO between the IS and LS states. Magnetic susceptibility measurements for the complexes with py and 4-CNpy showed gradual SCO in the temperature range of 300–100 K, and SCO in solution was also confirmed by ^{1}H NMR measurements for $[Fe^{III}(oetpp)(4\text{-}CNpy)_2]^+$.

Quite recently, Nakamura et al. reported an unprecedented SCO between HS and IS states in a highly saddled five-coordinated iron(III) porphyrin, $[Fe^{III}(OMTArP)(H_2O)]ClO_4$ (OMTArP = peripherally substituted octamethyltetraphenylporphyrin) [49]. Solid state EPR measurements suggested that $[Fe^{III}(OMTArP)(H_2O)]ClO_4$ is in the IS state above 20 K. The HS signal appeared at lower temperature region and an almost pure HS signal was observed at 1.5 K, suggesting SCO from IS to HS upon decreasing temperature. The SCO was confirmed by magnetic susceptibility measurements below 20 K. The authors ascribed this unprecedented SCO behavior to the highly saddled molecular structure and its crystal packing. The unit cell volume is expected to shrink as decreasing temperature and the shrinkage affects the molecular structure of porphyrin. The more saddled structure at lower temperature stabilizes HS states leading to SCO from IS to HS states.

2.5. Multi-nuclear iron(III) spin crossover complexes

Multi-nuclear SCO complexes are attractive from the view points of their multi-stability. SCO iron(III) complexes with quinquedentate Schiff-base ligands, [Fe(salten)(base)]$^+$ (base = heterocyclic ligands), are recognized as effective building units for preparing multi-nuclear SCO systems, because heterocyclic ligands coordinated to iron(III) ions from the axial position can be replaced by suitable bridging ligands [32].

Dinuclear iron(III) SCO compounds formulated as [(R-salten)Fe(bpy)Fe(R-salten)]$(BPh_4)_2$ (bpy = 4,4′-bipyridine) show very gradual SCO [50]. Gradual two step SCO was, on the other hand, observed in a binuclear complex of [(3-OMe-salten)Fe(vibpy)Fe(3-OMe-salten)]$(BPh_4)_2$ (vibpy = 1,2-bis(4-pyridyl)ethylene)) (Fig. 6a) [51]. The $\chi_m T$ - T plot for the dinuclear complex showed a stepped curve with plateaus at 350 K (7.70 emu mol^{-1} K) and 140 K (4.75 emu mol^{-1} K), suggesting SCO from HS–HS to HS–LS states on two iron(III) sites. Upon lowering temperature, the $\chi_m T$ values decreased gradually and reached a minimum value of 2.96 emu mol^{-1} K at 5 K. The magnetic data revealed that the dinuclear complex showed an incomplete two-step SCO from HS–HS to LS–LS through the intermediate HS-LS state. In X-ray structure analysis, two iron(III) ions bridged by vibpy ligands are crystallographically independent in the intermediate HS–LS state, and the two-step SCO is due to subsequent spin interconversions in two distinct iron(III) ions.

$[\{Fe(salten)\}_3Cr(CN)_6]$, prepared by the reaction of [Fe(salten)Cl] with $K[Cr(CN)_6]\cdot 2H_2O$, has three SCO sites of [Fe(salten)]$^+$ assembled by $[Cr(CN)_6]^{3-}$ with cyanide bridges (Fig. 6b) [52]. The Mössbauer and magnetic data for the tetranuclear complex were analyzed by considering magnetically interacting SCO moieties. Three iron(III) sites are magnetically coupled via hexacyano chromate, and the occurrence of multi-step SCO was suggested. An nonanuclear complex of $[\{Fe(3\text{-}EtO\text{-}salten)\}_8Mo(CN)_8]$ was also prepared by using $[Mo(CN)_8]^{4-}$ as a bridging unit and a gradual SCO was observed [53].

A SCO iron(III) complex of [Fe(acen)(L)]$^+$ (L = N-donating heterocyclic ligand) is a suitable building unit to prepare polynuclear systems. A reaction of [Fe(acen)Cl] with bpyp (bpyp = 1,3-bis(4-pyridyl)propane) in 1:1 ratio gave a 1D SCO iron(III) complex of $[Fe(acen)(bpyp)]_n(BPh_4)_n$ [54]. [Fe(acen)(L)]$^+$ units are bridged by the flexible bridging bpyp, forming a 1D chain. X-ray structure analyses showed the existence of two crystallographically independent iron(III) sites, each ion forming 1D chains. Both iron(III) ions are in the LS states at 108 K, and one of the iron(III) ions converts to the HS states at 180 K. At 296 K, both iron(III) ions become HS. The magnetic susceptibility measurements revealed that the 1D polynuclear complex exhibits a very gradual SCO behavior in the temperature range of 100–350 K.

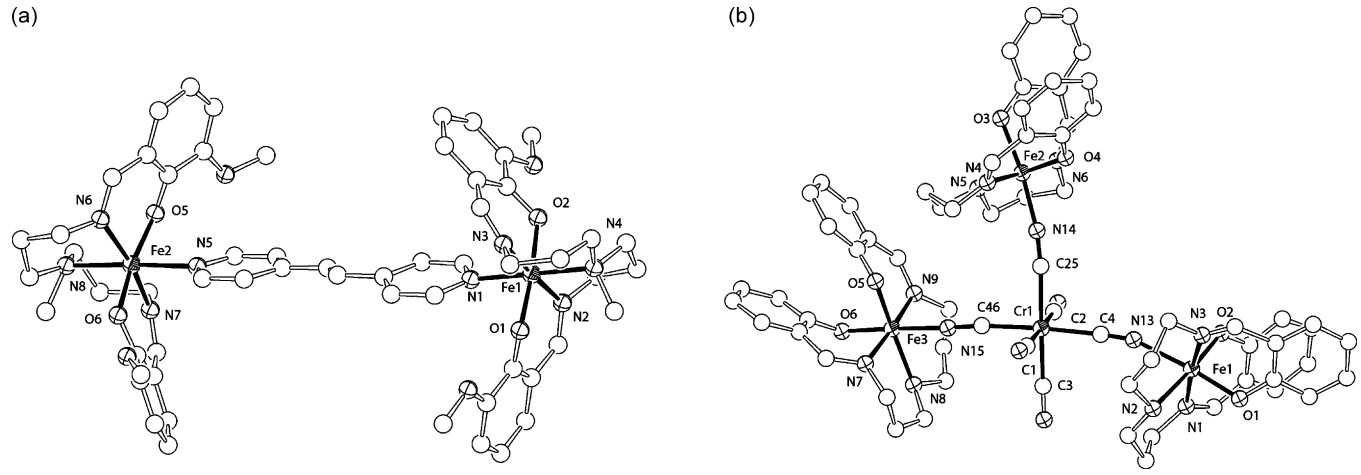

Fig. 6. Structures of (a) the cations in [(3-OMe-salten)Fe(vibpy)Fe(3-OMe-salten)]$(BPh_4)_2$, and (b) [{Fe(salten)}$_3$Cr(CN)$_6$] [51,52].

3. Physical properties of spin crossover iron(III) systems

3.1. Magnetic susceptibility and heat capacity measurements

SCO iron(III) complexes exhibit temperature variation of effective magnetic moments (μ_{eff}) upon spin interconversion from HS ($S = 5/2$) to LS ($S = 1/2$) states. Typical μ_{eff} values are 5.5–6.0 B.M. for the HS iron(III), while the LS iron(III) gives the effective magnetic moments of 2.0–2.3 B.M. Fig. 7 shows a μ_{eff} versus T plot for a typical SCO iron(III) complex, which shows a gradual decrease of the value from 5.7 BM at 320 K to 2.2 BM at 78 K. This magnetic behavior indicates a spin-equilibrium process between $^6A_1$ and $^2T_2$ states.

High-spin fractions (f_{HS}) were readily calculated by considering a simple additive property of magnetic susceptibilities:

$$\mu_{eff}^2 = f_{HS}\mu_{eff}(HS)^2 + (1 - f_{HS})(\mu_{eff}(LS)^2) \quad (1)$$

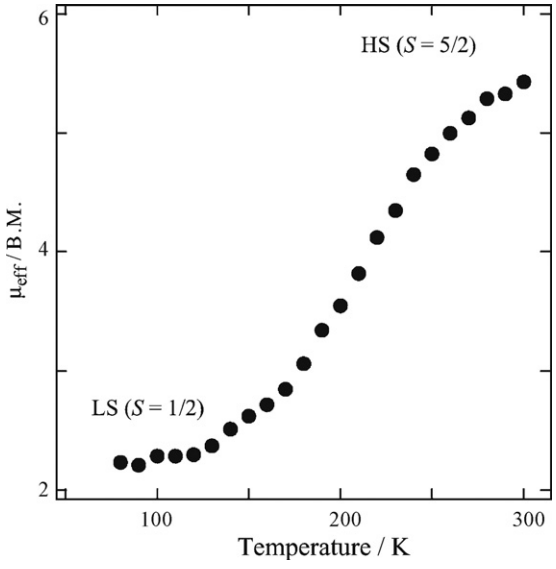

Fig. 7. Temperature dependences of magnetic moment (μ_{eff}) of a typical SE spin crossover compound.

where μ_{eff}(HS) and μ_{eff}(LS) are typical effective magnetic moments for the HS ($S = 5/2$) and LS ($S = 1/2$) states, respectively.

Heat capacity measurements revealed that SCO complexes have larger entropy changes upon spin transitions than the values calculated from the spin manifold changes, and the excess entropy changes are due to the lattice contributions. The enthalpy and entropy changes accompanied with the spin transition are given by $\ln K = -\Delta H/RT + \Delta S/R$, where the equilibrium constant is $K = f_{HS}/(1 - f_{HS})$. Experimentally obtained entropy changes for SCO iron(III) complexes are usually five times as large as the values expected for the magnetic contribution ($R \ln 3 = 9.1$ J K^{-1} mol^{-1}), and the extra entropy change was considered to come from lattice contribution. The separation energy (E) between zero-point levels of the HS and LS states is estimated by the analysis of temperature dependence of the magnetic moments (μ_{eff}) which is expressed by the molecular vibrational partition function as follows [55]:

$$\mu_{eff}^2 = \frac{\{0.75g^2 + 8x^{-1}[1 - \exp(-3x/2)] + 105C\exp[-(1 + E/\zeta)x]\}}{\{1 + 2\exp(-3x/2) + 3C\exp[-(1 + E/\zeta)x]\}} \quad (2)$$

where ζ is the one-electron spin–orbit coupling constant, C is the ratio of the molecular partition functions estimated from the equilibrium constant, and $x = \zeta/kT$. It is noted that some systems undergo the spin transition even in solution. [Fe(Him)$_2$(salacen)]$BPh_4 \cdot CH_3OH$ and [Fe(hapacen)(Him)$_2$]$BPh_4 \cdot 2CH_3OH$ are almost in the LS state in the solid state, but they show spin crossover in solution [39]. Solid [Fe(acac$_2$trien)]PF_6 is in the HS, while [Fe(acac$_2$trien)]BPh_4 and [Fe(sal$_2$trien)]$NO_3 \cdot H_2O$ are nearly in the LS state. These complexes exhibit SCO in solution, and their SCO behavior depends upon solvents and the substituent groups on chelate rings [42]. [Fe(sal$_2$3,3,3-tet)]NO_3 and [Fe(sal$_2$3,2,3-tet)]NO_3 are in the HS and LS states, respectively, the former showing the spin transition in methanol [56].

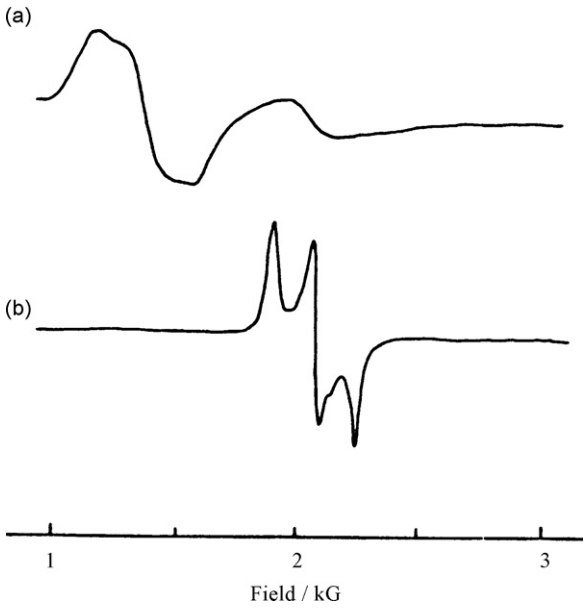

Fig. 8. EPR spectra of (a) HS and (b) LS species in SE compounds.

3.2. Absorption and EPR spectra

Reversible thermochromism accompanied with spin transitions is observed in SCO iron(III) complexes with FeN_4O_2 chromophores. Color is changed from green to blue, dark red, brown, violet or black upon spin transitions from the LS to the HS species. HS species show metal-to-ligand charge transfer bands at 500–550 nm (ε = 500–3500 dm^3 mol^{-1}), and upon the spin transition to the LS species the bands decrease steadily in intensity and the lower energy bands appear at 600–700 nm [8f].

EPR spectroscopy is a very useful tool to study electronic states of HS and LS species in SCO iron(III) systems. Typical EPR spectra for HS and LS species are displayed in Fig. 8. A LS Fe(III) ion under the O_h symmetry has a $^2T_{2g}$ state which splits into three Kramers doublets of ^2E and ^2A by molecular distortion and spin–orbit coupling. A ^6A state of the HS iron(III) also splits into three Kramers doublets, though their splitting is very small. The HS iron(III) ion gives broad EPR signal with the g values of ca. 2.1 and 4.1 (Fig. 8), and this anisotropy comes from the rhombic distortion of complex molecules. In LS iron(III) ions, on the other hand, the anisotropic g values of sharp signals can be used to analyze the nature of the ground state Kramers doublet (^2T state). Considering the $(t_2)^5$ configuration as $(t_2)^1$ configuration, the six spin–orbit distortion matrix eigenfunctions may be given as

$$\phi_i^+ = A_i|1^+\rangle + B_i|\zeta_1^-\rangle + C_i|-1^+\rangle,$$
$$\phi_i^- = A_i|-1^-\rangle - B_i|\zeta_1{}^+\rangle + C_i|1^-\rangle$$
$$\left(i = 1, 2, 3, \quad \zeta_1 = \frac{1}{\sqrt{2}}\{|2\rangle - |-2\rangle\}\right)$$

where ζ is spin–orbit coupling constant. The g values for LS iron(III) ions are derived as [8d,57]:

$$g_z = 2[A^2 - B^2 + C^2 + k(A^2 - C^2)],$$
$$g_x = 2[B^2 - 2AC + \sqrt{2}kB(A - C)],$$
$$g_y = 2[B^2 + 2AC + \sqrt{2}kB(A - C)]$$

where k is the orbital reduction factor and usually fixed to 0.9. The values of A, B and C are determined by using the anisotropic g values. It is noted that the sign of the g values cannot be experimentally determined and a reasonable one should be chosen in some solutions. The large value of B_1 compared with the others means that the ground state Kramers doublet consists mainly of the state with unpaired electrons on the d_{xy} orbital and that the sign of the electric field gradient is negative. The spin orbit coupling constant and the crystal field distortion parameters can be determined by using the Hamiltonian:

$$H = -\zeta \mathbf{l}\cdot\mathbf{s} - \delta(\mathbf{l}_z^2 - 2)\frac{\varepsilon}{2}(\mathbf{l}_+^2 + \mathbf{l}_-^2) \quad (3)$$

where δ and ε are tetragonal and orthorhombic distortion parameters, respectively, and the δ/ζ and ε/ζ values can be determined by using the A_1, B_1, and C_1 values. EPR parameters can be used to characterize the electronic structure of SCO iron(III) systems. The LS species in [Fe(acen)(lut)$_2$]BPh4 and [Fe(acpa)$_2$]PF_6 have g = 2.389, 2.310, 1.901 and g = 1.954 and 2.220, respectively. [Fe(salAPA)$_2$]ClO_4 with trans geometry exhibits rhombic signals at g = 2.349, 2.109, and 1.951 [24]. Tetragonally distorted complexes in the LS state have the ground state of either ^2E or ^2A state arising from an octahedral ^2T state. In a series of [FeL(Him)$_2$]$^+$ (L = acen, hapacen, and salacen), [Fe(acpa)$_2$]$^+$, [Fe(salAPA)$_2$]$^+$, and [Fe(salEen)$_2$]$^+$, EPR measurements revealed that the unpaired electrons on the LS iron(III) ions stayed in the d_{xy} orbital.

3.3. Mössbauer spectra

Mössbauer parameters of isomer shift (δ) and quadrupole splitting (ΔE) are very sensitive to environment about iron ions, and they are used to characterize oxidation and spin states of iron ions. Iron(III) compounds in the HS state show a quadrupole doublet with δ = 0.25–0.37 mm s^{-1} relative to metallic iron and ΔE values are relatively small (<0.5 mm^{-1}). LS iron(III) compounds have, on the other hand, δ values in the range of 0.05–0.20 mm s^{-1} and relatively large ΔE values of 1.9–3.0 mm s^{-1}. Note that Mössbauer spectroscopy is a powerful tool to study dynamic electronic states with the time scale of 10^{-6}–10^{-8} s. SE systems interconvert their spin states with different rate constants. When the spin interconversion is slower than the Mössbauer time scale, two sets of quadrupole doublets corresponding to the HS and LS species are observed in the Mössbauer spectra. When the spin interconversion is much faster, the two sets of doublets cannot be resolved anymore and a single quadrupole doublet is observed. In rapid spin interconversion, the values of quadrupole splitting and isomer shift for the single doublet vary depending upon the fraction of each spin state. If the spin interconversion rate is comparable to the Mössbauer time scale, the Mössbauer spectra show a broadened quadrupole doublet, a so-called relaxation spectrum.

Mössbauer spectra can be used to estimate the relaxation time τ ($=\tau_{LS}\tau_{HS}/(\tau_{LS}+\tau_{HS})$ from HS to LS states, where τ_{LS} and τ_{HS} represent the lifetime of LS and HS states, respectively. Assuming the principal component of an axially symmetric electric field gradient jumping at random between LS and HS states, the time dependent Hamiltonian can be expressed as follows [58]:

$$H(t) = H_0 + (1 + f(t))\frac{\Delta_{HS}}{12}(3I_z^2 - I^2) + (1 - f(t)) \times \frac{\Delta_{LS}}{12}(3I_z^2 - I^2) \quad (4)$$

where the random function of time $f(t)$ is ± 1, and the Δ_{HS} and Δ_{LS} are the quadrupole splittings of HS and LS states, respectively. The theoretical Mössbauer spectrum has a form of

$$I(\omega) = \sum_i K \left\{ \frac{(1 + \tau\Gamma)P_i + Q_i R_i}{P_i^2 + R_i^2} \right\} \quad (5)$$

$$P_i = \tau[\Gamma^2 - \{\tfrac{1}{2}(\omega_i^h + \omega_i^l) - \omega^2\} + \tfrac{1}{4}(\omega_i^h - \omega_i^l)^2 + \Gamma],$$

$$Q_i = \tau\{\tfrac{1}{2}(\omega_i^h + \omega_i^l) - \omega - \tfrac{1}{2}(p_h - p_l)(\omega_i^h - \omega_i^l)\},$$

$$R_i = \{\tfrac{1}{2}(\omega_i^h + \omega_i^l)(1 + 2\tau\Gamma) + \tfrac{1}{2}(p_h - p_l)(\omega_i^h - \omega_i^l)\}$$

where the subscript i refers to an individual Mössbauer transition, the constant K is the relative intensity of the ith transition, and p_h and p_i are the populations of the HS and LS species, respectively [58].

Fig. 9 shows typical ^{57}Fe Mössbauer spectra for SCO iron(III) complexes [8d]. $[Fe(acpa)_2]X$ (X = BPh_4 and PF_6) have only one quadrupole doublet both at 77 and 300 K, each assigned to LS and HS species, respectively. In the intermediate temperature range, the PF_6^- salt gives two quadrupole doublets of the LS and HS species, while the BPh_4^- salt shows only one quadrupole doublet at the whole temperature range measured. In the BPh_4^- salt the spin-state interconversion between the HS and LS states is more rapid than the Mössbauer time scale ($>10^7$ s^{-1}), and the two quadrupole doublets of HS and LS species fuse into one. The asymmetry depends upon the fraction of HS and LS species. The analyses of Mössbauer spectra gave relaxation times of 6.9×10^{-7} to 1.6×10^{-5} s and 1.9×10^{-6} to 3.4×10^{-5} s for the PF_6^- and BPh_4^- salts, respectively. Detailed discussion of the spin interconversion process has been done by the classical activated complex theory [59].

3.4. Structural changes

Iron ions in the HS state have unpaired electrons on the antibonding e_g orbitals, while iron ions in the LS state have vacant e_g orbitals. The coordination bond lengths of the HS species are, therefore, longer than those of the LS species. ST type SCO complexes sometimes show spin interconversion accompanied with the first order phase transition, while SE type SCO complexes do not show drastic structural changes such as space group changes [60]. The difference in ΔFe–L values for SCO iron(III) complexes is smaller than those for SCO iron(II) complexes. SCO iron(II) complexes with FeN_6 chromophore show ca. 0.2 Å differences in bond lengths as the spin interconversion from HS to LS states. In SCO iron(III) complexes with N_4O_2 coordination, relatively large bond length changes (0.15 Å) are observed for Fe–N bonds, while the changes (0.04 Å) of Fe–O bonds are small (Table 1).

3.5. General consideration on rapid spin interconversion of LS state

In SCO iron(III) complexes, the ground LS state is the $^2T_{2g}$ under O_h symmetry and the $^6A_{1g}$ state becomes the ground state of HS. The spin interconversion occurs by virtue of the dominant entropy term in the Gibbs free energy. The question is raised as to why the spin transitions occur gradually in the SE type complexes. Heat capacity measurements for SE type complexes revealed that the number of molecules in a cell or a domain (domain size) was about 5 [61]. This value is extremely small compared with the values (95 and 77) estimated for ST type iron(II) SCO complexes such as $[Fe(phen)_2(NCS)_2]$ and $[Fe(phen)_2(NCSe)_2]$ [2h,2i]. The small domain size for SE type iron(III) SCO complexes, meaning less cooperativity and less intermolecular interactions, results in each molecule independently interconverting its spin state, hence, the spin interconversion occurs within a wide temperature range.

Some iron(III) SE type complexes have rapid spin interconversion rate compared with ^{57}Fe Mössbauer time scale, giving a single quadrupole doublet in the Mössbauer spectra even at the spin transition temperatures. The next question is why some SE type iron(III) complexes do show a rapid spin interconversion and others do not. There are three factors which might be responsible for the rapid spin interconversion. (i) A strong interaction between $^2T_{2g}$ and $^6A_{1g}$ states through an excited $^4T_{1g}$ state. (ii) Some vibrational modes with anharmonicity, which may affect the effectiveness of nuclear tunnelling. (iii) Structural difference such as reduced metal–ligand bond lengths between two-spin states. In this section we address the third factor to explain the rapid interconversion behavior by using structural parameters for $[Fe(acpa)_2]X$ (X = BPh_4 and PF_6), where the BPh_4^- salt shows more rapid spin interconversion than the PF_6^- salt. Temperature dependence of the X-ray analyses revealed that the degree of bond length changes for the faster spin interconversion complex, BPh_4^- salt, is smaller than that of the more slowly interconverting PF_6^- salt; $\Delta Fe–O_{av}$: 0.024 Å; $\Delta Fe–N(pyridine)_{av}$: 0.131 Å; $\Delta Fe–N(imine)_{av}$: 0.114 Å for the BPh_4^- salt and ΔFe–O: 0.042 Å; $\Delta Fe–N(pyridine)_{av}$: 0.170 Å; $\Delta Fe–N(imine)_{av}$: 0.145 Å for the PF_6^- salt. Let us describe potential surfaces of ground (LS state: $^2T_{2g}$) and excited (HS state: $^6A_{1g}$) states as single parabolic functions (Fig. 10). The magnetic susceptibility measurements show that the HS fraction of the PF_6^- salt is always higher than that of the BPh_4^- salt at any temperature. The HS state ($^6A_{1g}$) for the PF_6^- salt is always placed below the $^6A_{1g}$ state of the BPh_4^- salt, assuming both complexes having the ground LS state ($^2T_{2g}$) in the same energy. Taking the longer HS bond lengths for the PF_6^- salt than those for the BPh_4^- salts into account, the potential surface of the $^6A_{1g}$ state for the PF_6^- salt is placed further from the $^2T_{2g}$ state

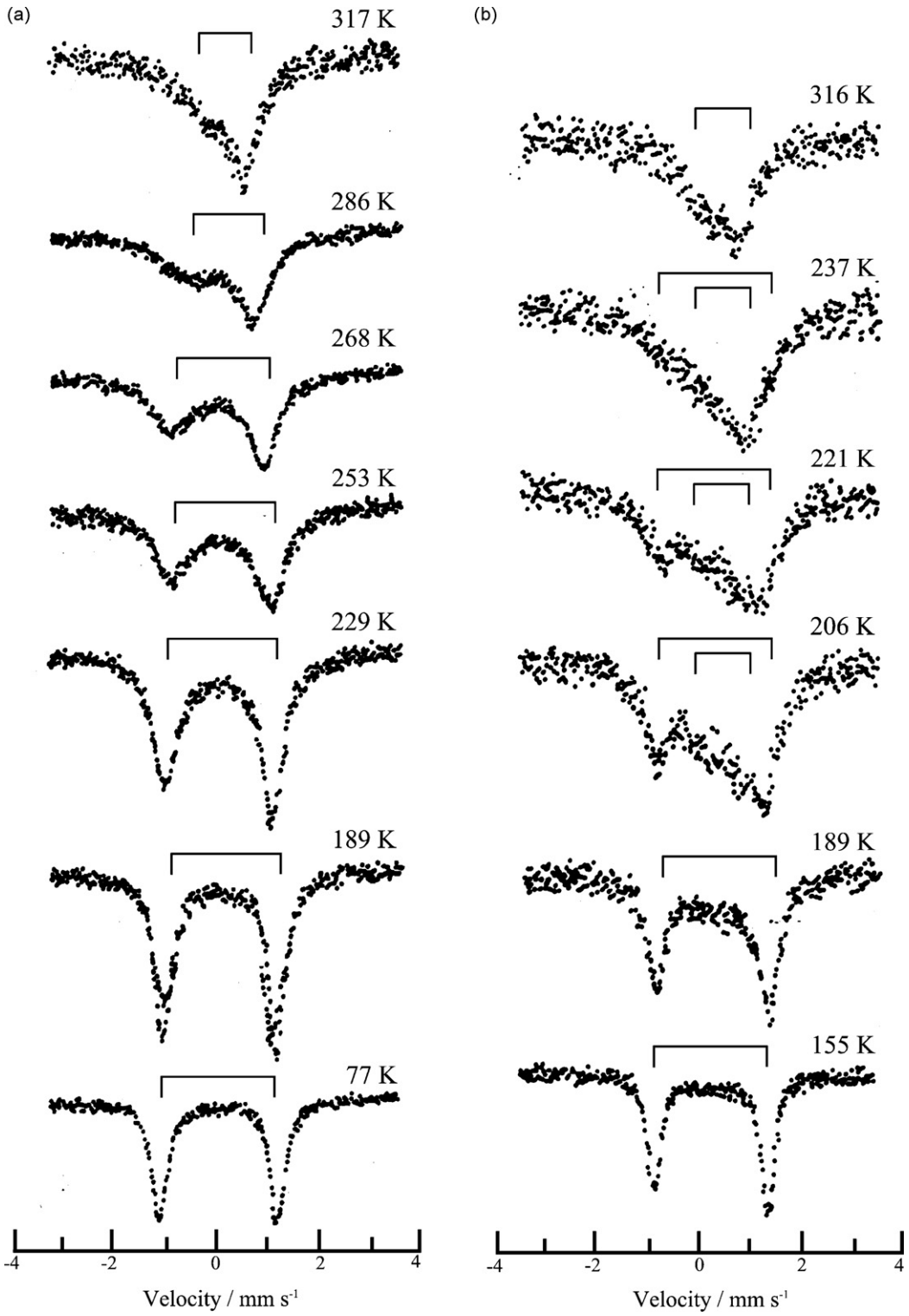

Fig. 9. Mössbauer spectra of (a) $[Fe(acpa)_2]BPh_4$ and (b) $[Fe(acpa)_2]PF_6$.

than that of the BPh_4^- salt (Fig. 10). The activation energy ΔE_a of the spin interconversion for the PF_6^- salt is, therefore, larger than that for the BPh_4^- salt. From the Arrhenius' equation, the rate constant k for the spin interconversion can be related to the activation energy ΔE_a as $k = A\exp(-\Delta E_a/RT)$, where A and R are the frequency factor and the gas constant, respectively. According to the above arguments, the activation energy ΔE_a of the BPh_4^- salt can be expected to be smaller than that of the PF_6^- salt, hence, the smaller ΔE_a value for the BPh_4^- salt supports its more rapid spin interconversion compared with the PF_6^- salt. It is noted that rate constants of spin interconversion rates in both solution and solid states have been determined in

Table 1
Coordination bond lengths (Å) of HS and LS species and their differences (Å) in SCO iron(III) complexes with Schiff-base ligands[a]

	HS–LS			Differences in bond lengths			Reference
	Fe–O	Fe–O	Fe–O	ΔFe–O	ΔFe–Npy	ΔFe–Nim	
$[Fe(acpa)_2]BPh_4$	1.916 (1.920)	2.088 (2.113)	2.028 (2.052)	0.020 (0.024)	0.106 (0.131)	0.090 (0.114)	[3e]
	1.896	1.982	1.938				
$[Fe(acpa)_2]PF_6$	1.939 (1.941)	2.153 (2.159)	2.081 (2.086)	0.040 (0.042)	0.164 (0.170)	0.140 (0.145)	[3e]
	1.899	1.989	1.941				
$[Fe(bzpa)_2]ClO_4$	1.921	2.074	2.017	0.013	0.098	0.097	[11]
	1.908	1.976	1.920				
[Fe(acen)(3,4-lut)$_2$]	1.929	2.185	2.057	0.023	0.149	0.139	[11]
BPh_4	1.906	2.036	1.918				
[Fe(3OEt-salAPA)]	1.921	2.176	2.085	0.064	0.148	0.128	[2l]
ClO_4	1.857	2.028	1.957				
[Fe(im)$_2$(salen)]	1.901	2.146	2.067	−0.002	0.154	0.154	[3f]
ClO_4	1.903	1.992	1.913				
[Fe(3-al-salBzen)$_2$]	1.896	2.121	1.982				[3e]
NO_3	1.883	2.047	1.936				

[a] The values in the parentheses are obtained by the linear extrapolation to the 100% HS species. The HS fractions are estimated from the magnetic susceptibility data.

some ferric SCO complexes [62] and that the spin interconversion in solution is much faster than that of corresponding solid samples. Furthermore, grinding and dilution experiments for the ferric spin crossover complexes revealed that such physical treatments affect the dynamics of the spin crossover phenomena [3b,63].

3.6. Cooperativity and photo-induced spin transition in spin crossover iron(III) system

Spin interconversion by light irradiation was firstly observed in a SCO iron(II) system, and this was named 'LIESST' (Light Induced Excited Spin State Trapping) [64]. In some SCO Fe(II) complexes, the thermally stable LS state was converted to the HS state by light irradiation, and the light induced HS state maintained at low temperature to prevent back interconversion of spin states. In SCO iron(II) and iron(III) complexes, coordination bond distances change with spin interconversion. The average bond distance change for SCO iron(II) compounds is 0.18 Å [65], while the smaller changes (0.12 Å) were observed in SCO Fe(III) compounds. It is, therefore, presumed that the life-time of the photo-induced excited HS state for SCO iron(III) complexes is shorter than that for SCO Fe(II) complexes, because the fast back spin interconversion to the LS state occurs due to the smaller activation energy from metastable HS to LS states in SCO iron(III) complexes. Note that the occurrences of a transient HS species of the iron(III) complex in solution was firstly reported by McGarvey et al. [66].

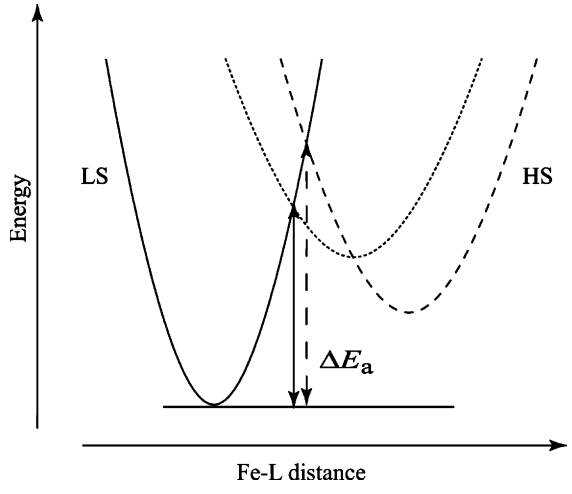

Fig. 10. Schematic representation of the structural change influence on the LS and HS potential wells in SCO complexes. The dashed and dotted lines correspond to the HS potential wells for PF_6^- and BPh_4^- salts, respectively.

Although LIESST is unfavorable in SCO iron(III) systems, introduction of strong intermolecular interactions such as π-stacks and hydrogen bonds afford cooperative spin interconversion with large thermal hysteresis and LIESST effects. The first LIESST effect in solid was observed in $[Fe(pap)_2]ClO_4{\cdot}H_2O$ [21], which exhibits abrupt transition at $T_{1/2}\uparrow = 180$ K and $T_{1/2}\downarrow = 165$ K. X-ray crystal structure analyses revealed that $[Fe(pap)_2]ClO_4{\cdot}H_2O$ showed large structural changes upon SCO compared with that in typical iron(III) SCO complexes and strong intermolecular π-stacks of aromatic rings in pap^- were observed. The large structural change upon SCO and strong intermolecular interactions caused strong cooperativity and abrupt SCO behaviors. Light irradiation of the LMCT band (400–600 nm) generates the meta-stable HS species, and the species retain up to about 100 K, suggesting an occurrence of LIESST. $[Fe(pap)_2]PF_6{\cdot}MeOH$ also showed thermally induced abrupt SCO without hysteresis at 288 K, and LIESST was observed below 55 K [21]. Further example of LIESST was reported for [Fe(thpu)(Hthpu)], where H_2thpu is a tridentate Schiff base derived from a condensation of pyruvic acid with thiosemicarbazide) [67]. [Fe(thpu)(Hthpu)] exhibited abrupt SCO with hysteresis ($T_{1/2}\uparrow = 239$ K and $T_{1/2}\downarrow = 225$ K), which is attributed to hydrogen bond network, and the LIESST effect was observed below 40 K.

$[Fe(qsal)_2(NCSe)_2]\cdot MeOH$, which has significant intermolecular π-π interactions, showed one of the largest hysteresis ($\Delta T_{1/2} = 70$ K) upon SCO [68]. $Li[Fe(5\text{-Br-thsa})_2]\cdot H_2O$ ($H_2$5-Br-thsa = 5-bromosalicylaldehyde thiosemicarbazone) with strong hydrogen bond networks showed SCO accompanied with large hysteresis ($\Delta T_{1/2} = 39$ K) due to a crystallographic first-order phase transition [69]. Although LIESST effects in $[Fe(qsal)_2(NCSe)_2]\cdot MeOH$ and $Li[Fe(5\text{-Br-thsa})_2]\cdot H_2O$ have not been observed so far, they are possible candidates exhibiting LIESST.

Relaxation dynamics for a metastable HS state generated by LIESST were studied by means of IR spectroscopy for a SCO iron(III) complex, $[Fe(cat)(tpa)]BPh_4$ (cat = catechol) [70]. $[Fe(cat)(tpa)]BPh_4$ dispersed in KBr showed partial generation of transient HS state by light irradiation below 50 K, and the relaxation rate constant (k_{HL}) of the transient HS states was estimated to be 0.58 s^{-1}. $[Fe(acpa)_2]PF_6$ and $[Fe(sal_2trien)]PF_6$ were gradual SCO systems, and their k_{HL} values in the same experimental conditions were estimated to be 3.9×10^2 and 1.9×10^2 s^{-1}, respectively, which is significantly larger than that for $[Fe(cat)(tpa)]BPh_4$. The striking difference in the relaxation dynamics was attributed to charge transfer interactions between metal ion and non-innocent catecholate ligands. Note that the k_{HL} value for $[Fe(pap)_2]PF_6$, exhibiting the long-lived HS state by LIESST, is about 10^{-3} s^{-1}.

An introduction of potentially photo-isomerizable ligands into SCO iron(III) systems gives a different type of light induced SCO behavior. The inclusion of structurally isomarizable ligands in Fe(III) SCO complexes may affect the spin-state conversion. This phenomenon is known as LD-LISC. $[Fe(salten)(base)]BPh_4$ systems, which have photo-isomerizable heterocyclic ligands, exhibited interesting photo-responsive SCO behavior. $[Fe(salten)(Mepepy)]BPh_4$ (Mepepy = 1-(pyridine-4-yl)-2-(N-methylpyrrol-2-yl)-ethene) showed a gradual SCO when Mepepy is in the trans form [71]. Photo-isomarization from trans to cis form of Mepepy in acetonitrile at room temperature affords partial spin conversion to the HS state.

3.7. Synergy of spin crossover and other physical properties

A new class of SCO iron(III) systems, which have other functions such as magnetism and conductivity, are currently attracted much research interest. SCO iron(III) complexes change not only structure but also electronic- and magnetic properties during SCO. Introduction of other functional systems into SCO complexes may lead to synergistic effects by possible structural and magnetic perturbations. Recent progress toward new SCO iron(III) systems is presented in this section.

$MnPS_3$ is a layered compound and reactions with ionic salts (G^+X^-) yield intercalated ferromagnetic materials formulated as $G_{2x}Mn_{1-x}PS_3\cdot$(solv.) [72]. Intercalation of a SCO iron(III) complex, $[Fe(5\text{-OMe-sal}_2trien)]^+$, into the $MnPS_3$ host lattice yielded $[Fe(5\text{-OMe-sal}_2trien)]_{0.28}Mn_{0.86}PS_3\cdot nH_2O$ [73]. This material exhibited thermal SCO of the guest molecules and ferrimagnetic ordering of the host lattice. Note that a synergistic behavior of simultaneous ferromagnetic ordering and thermal SCO has not been so far observed.

SCO iron(III) complexes with organic radicals are good candidates for the systems exhibiting synergy of SCO and magnetic interactions. A ferric complex with organic radicals, $[Fe(L)_3]$ (L = butyl-substituted *o*-iminobenzosemiquinonate radical) showed thermally induced SCO (Fig. 11) [74]. At

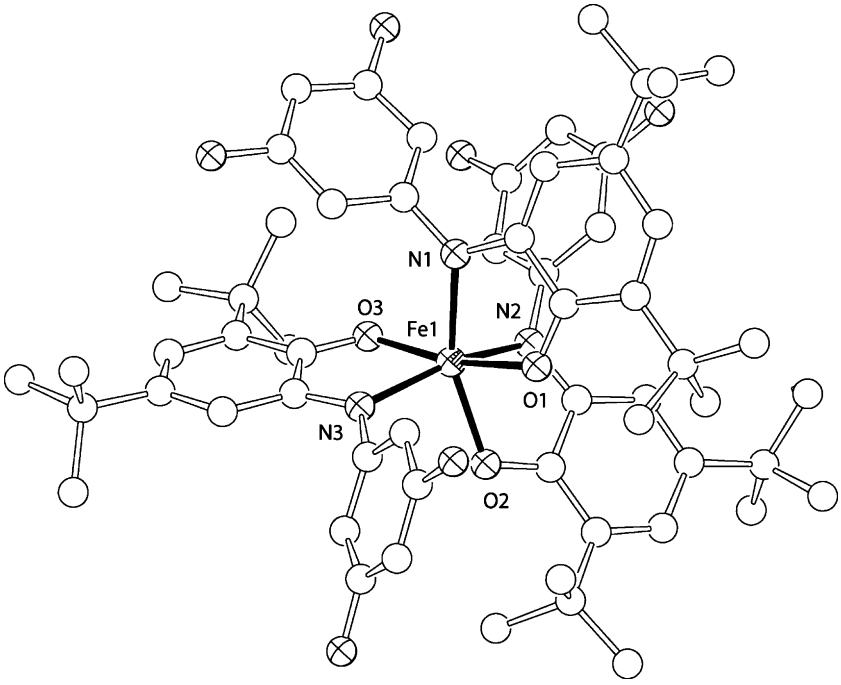

Fig. 11. Structure of $[Fe(L)_3]$ (L = butyl-substituted o-iminozenzosemiquinonate radical) [74].

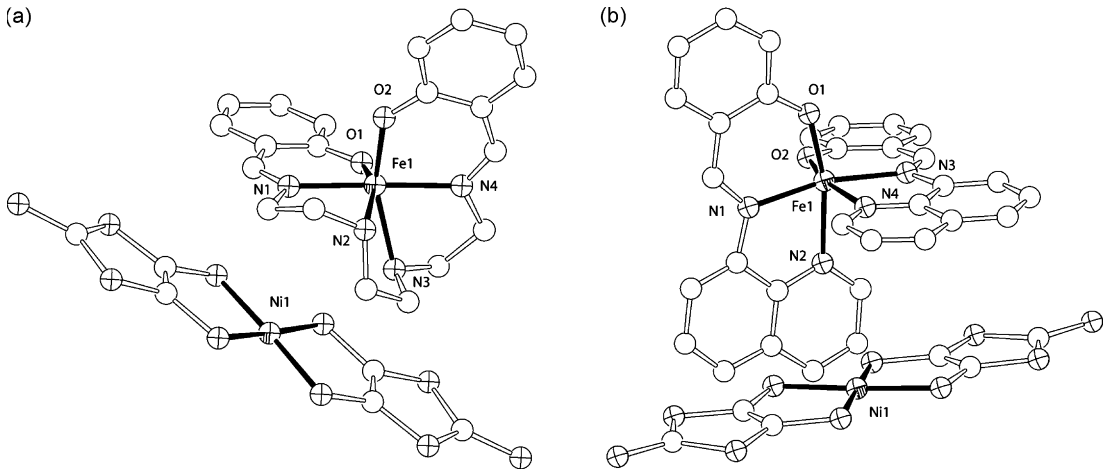

Fig. 12. . Structures of (a) $[Fe(sal_2trien)][Ni(dmit)_2]_2$, and (b) $[Fe(qsal)_2][Ni(dmit)_2]_2{\cdot}2CH_3CN$ [75,76].

low temperature $[Fe(L)_3]$ has a LS iron(III) ion and three spin-frustrated semiquinone radicals, leading to a diamagnetic ground state. In high temperature region, on the other hand, antiferromagnetic interactions between the central iron(III) ion ($S = 5/2$) and three radicals lead to $S = 1$ spin ground state.

Partially-oxidized $[Ni(dmit)_2]^{n-}$ salts (dmit = 4,5-dithiolato-1,3-dithiole-2-thione) are representative conductive materials, and they give molecular semi-conductors, metals, and super-conductors. Combination of cationic SCO iron(III) complexes and $[Ni(dmit)_2]^{n-}$ salts may give materials with controllable conductivity by external stimuli. The first SCO iron(III) complex with $[Ni(dmit)_2]^{n-}$ salts, formulated as $[Fe(sal_2trien)][Ni(dmit)_2]$, was reported by Faulmann et al. [75] (Fig. 12a). $[Fe(sal_2trien)][Ni(dmit)_2]$ is an insulator, and the compound exhibits cooperative SCO ($T_{1/2}\uparrow = 258$ K and $T_{1/2}\downarrow = 228$ K $\Delta T_{1/2} = 30$ K). In $[Fe(sal_2trien)][Ni(dmit)_2]$, no intermolecular interactions were observed between complex cations and $[Ni(dmit)_2]^{1-}$ salts, and the large cooperativity is operative via intermolecular π–π interactions between neighboring aromatic rings in sal_2trien^{2-}. $[Fe(qsal)_2][Ni(dmit)_2]{\cdot}2CH_3CN$ is the second example (Fig. 12b) [76]. Each $[Fe(qsal)_2]^+$ and $[Ni(dmit)_2]^-$ formed 1D chains by π–π and S···S interactions, respectively, and they were separated by solvent molecules. 1D $[Fe(qsal)_2]^+$ showed abrupt SCO with hysteresis ($T_{1/2}\uparrow = 231$ K and $T_{1/2}\downarrow = 194$ K) and a LIESST effect was confirmed below 46 K. A partially oxidized compound, formulated as $[Fe(qsal)_2][Ni(dmit)_2]_3{\cdot}CH_3CN{\cdot}H_2O$, was prepared by electrolysis of $[Fe(qsal)_2][Ni(dmit)_2]{\cdot}2CH_3CN$ [77]. $Ni(dmit)_2$ molecules stack alongside each other with face-to-face alignments and form 1D chains. $[Fe(qsal)_2][Ni(dmit)_2]_3{\cdot}CH_3CN{\cdot}H_2O$ is a semiconductor and the resistivity curve shows an anomaly with hysteresis in the temperature range of 90–120 K. It is noteworthy that a magnetic hysteresis loop was also observed in the SCO profile in the same temperature range. The observed results suggested the possible existence of synergy between SCO and electric conductivity.

4. Conclusion

X-ray structural and magnetic studies on SCO iron(III) complexes were presented and the origin of the rapid spin interconversion was discussed. SCO Iron(III) complexes were classified into two types, namely, ST and SE types, and the different SCO behaviors can be understood by the domain model. The larger domain size leads to the ST type and the abrupt spin transition between HS and LS occurs. The SE type systems show gradual spin transition due to the smaller domain size, some of which show rapid spin interconversion. SCO complexes have been recognized as a good candidate for switching devices, because they exhibit SCO as a result of external stimuli such as heat, pressure, magnetic field and light. Synergy of SCO, magnetism, and electric conductivity may give new physical properties and can be applied to new molecular switching devices.

Acknowledgements

This work was partially supported by a Grant-in-aid for Scientific Researches from the Ministry of Education, Culture, Sports, Science and Technology, Japan, and by and TARA projects of university of Tsukuba.

References

[1] L. Cambi, A. Cagnasso, A. Atti, Accad. Naz. Lincei, Cl. Sci. Fis. Mat. Nattl., Rend. 13 (1931) 809.
[2] (a) P. Adler, L. Wiehl, E. Meissner, C.P. Köhler, H. Spiering, E. Meissner, P. Gütlich, J. Phys. Chem. Solids 48 (1987) 517;
(b) M. Sorai, J. Ensling, P. Gütlich, Chem. Phys. Lett. 18 (1976) 199;
(c) H. Köppen, E.W. Müller, C.P. Köhler, H. Spiering, E. Meisssner, P. Gütlich, Chem. Phys. Lett. 91 (1982) 348;
(d) P. Gütlich, Struct. Bond. 44 (1981) 83;
(e) E. König, G. Ritter, S.K. Kulshreshtha, Chem. Rev. 85 (1985) 219;
(f) E. König, K. Madeja, Inorg. Chem. 6 (1967) 48;
(g) E. König, G. Ritter, S.K. Kulshreshtha, S.M. Nelson, J. Am. Chem. Soc. 105 (1983) 1924;
(h) M. Sorai, S. Seki, J. Phys. Soc. Jpn. 33 (1972) 575;
(i) M. Maeda, Y. Takashima, Y. Nishida, Bull. Chem. Soc. Jpn. 49 (1976) 2427;

(j) A.M. Greenaway, E. Sinn, J. Am. Chem. Soc. 100 (1978) 8080;
(k) A.M. Greenaway, C.J. O'Connor, A. Schrock, E. Sinn, Inorg. Chem. 18 (1979) 2692;
(l) B.A. Katz, C.E. Strouse, J. Am. Chem. Soc. 101 (1979) 6214.
[3] (a) M.S. Hadad, M.W. Lynch, W.D. Federer, D.N. Hendrickson, Inorg. Chem. 20 (1981) 123;
(b) W.D. Federer, D.N. Hendrickson, Inorg. Chem. 23 (1984) 3870;
(c) M.D. Timken, C.E. Strouse, S.M. Soltis, S.R. Daverio, D.N. Hendrickson, A.M. Abdel-Mawgoud, S.A. Wilson, J. Am. Chem. Soc. 108 (1986) 395;
(d) G. Sim, E. Sinn, R.H. Petty, C.L. Merrill, L.J. Wilson, J. Inorg. Chem. 20 (1981) 213;
(e) H. Oshio, K. Toriumi, Y. Maeda, Y. Takashima, Inorg. Chem. 30 (1991) 4252;
(f) K. Kaji, M. Sorai, Thermochim. Acta 88 (1985) 185.
[4] (a) P. Gülichi, H.A. Goodwin (Eds.), Spin Crossover in Transition Metal Compounds I–III, Springer, Top. Curr. Chem. 233–235 (2004);
(b) J.A. Real, A.B. Gaspar, V. Niel, M.C. Muñoz, Coord. Chem. Rev. 236 (2003) 121;
(c) J.A. Real, A.B. Gaspar, M.C. Muñoz, Dalton Trans. (2005) 2062;
(d) P. Gütlich, A. Hauser, H. Spiering, Angew. Chem. Int. Ed. Engl. 33 (1994) 2024.
[5] T. Kambara, Chem. Phys. 70 (1979) 4199.
[6] (a) T. Sasaki, T. Kambara, J. Chem. Phys. 74 (1981) 3472;
(b) T. Kambara, J. Chem. Phys. 74 (1981) 4557.
[7] (a) C.P. Slichter, H.G. Drickamer, J. Chem. Phys. 56 (1972) 2142;
(b) H. Köppen, E.W. Müller, C.P. Köhler, H. Spiering, E. Meissner, P. Gütlich, Chem. Phys. Lett. 91 (1982) 348;
(c) M. Sorai, S. Seki, J. Phys. Chem. Solids 35 (1974) 555.
[8] (a) M.D. Timken, A.M. Abdel-Mawgoud, D.N. Hendrickson, Inorg. Chem. 25 (1986) 160;
(b) Y. Nishida, S. Oshio, S. Kida, Bull. Chem. Soc. Jpn. 50 (1977) 199;
(c) B.J. Kennedy, A.C. McGrath, K.S. Murray, B.W. Skelton, A.H. White, Inorg. Chem. 26 (1987) 483;
(d) H. Oshio, Y. Maeda, Y. Takashima, Inorg. Chem. 22 (1983) 2684;
(e) H. Oshio, K. Kitazaki, K.J. Mishiro, N. Kato, Y. Maeda, Y. Takashima, J. Chem. Soc. Dalton Trans. (1987) 1341;
(f) Y. Maeda, N. Tsutsumi, Y. Takashima, Inorg. Chem. 23 (1984) 2440.
[9] P.B. Merrithew, P.G. Rasmussen, Inorg. Chem. 11 (1972) 325.
[10] K.R. Kunze, D.L. Perry, L.J. Wilson, Inorg. Chem. 16 (1977) 594.
[11] D. DeFilipo, P. Depalano, A. Diaz, S. Steffe, E.F. Trogu, J. Chem. Soc. Dalton (1977) 1566.
[12] (a) D.K. Greiger, Y.J. Lee, W.R. Scheidt, J. Am. Chem. Soc. 106 (1984) 6339;
(b) W.R. Scheidt, S.R. Osvath, Y.J. Lee, C.A. Reed, C.A.B. Shaevitz, G.P. Gupta, Inorg. Chem. 28 (1989) 1591.
[13] P.J. van Koningsbruggen, Y. Maeda, H. Oshio, in: P. Gütlich, H.A. Goodwin (Eds.), Spin Crossover in Transition Metal Compounds, vol. I, Springer, Top. Curr. Chem. 233 (2004) 167.
[14] (a) L. Cambi, L. Szegö, Ber 10 (1931) 2591;
(b) L. Cambi, L. Szegö, Ber 66 (1933) 656.
[15] (a) J. Albertsson, Å. Oskarssonk, Acta Crystallogr. B33 (1977) 1871;
(b) J. Albertsson, Å. Oskarssonk, Acta Crystallogr. B35 (1979) 1473;
(c) S. Mitra, C.L. Ratson, A.H. White, Aust. J. Chem. 29 (1976) 1899;
(d) J. Albertsson, I. Elding, Å. Oskarssonk, Acta Chem. Scand. A33 (1979) 703;
(e) M. Sorai, J. Inorg. Nucl. Chem. 40 (1978) 1031;
(f) K.B. Pandeya, R. Singh, C. Prakash, J.S. Baijal, Solid State Commun. 64 (1987) 801;
(g) A. Malliaris, V. Papaefthimiou, J. Chem. Phys. 74 (1981) 3626;
(h) G.R. Hall, D.N. Hendrickson, Inorg. Chem. 15 (1976) 607;
(i) C. Flick, E. Gelerinter, Chem. Phys. Lett. 23 (1973) 422.
[16] J. Albertsson, Å. Oskarsson, K. Stahl, Acta Chem. Scand. A36 (1982) 783.
[17] (a) H. Nakajima, T. Takana, H. Kobayashi, I. Tsujikawa, Inorg. Nucl. Chem. Lett. 12 (1976) 689;
(b) J. Ahmed, J.A. Ibers, Inorg. Chem. 16 (1977) 935.
[18] S. Hayami, T. Kawahara, G. Juhasz, K. Kawamura, K. Uehashi, O. Sato, J. Am. Chem. Soc. 123 (2001) 11644.
[19] (a) B.M. Dahl, O. Dahl, Acta Chem. Scand. 23 (1969) 1503;
(b) R.C. Dickinson, W.A. Baker Jr., R.L. Collins, J. Inorg. Nucl. Chem. 39 (1977) 1531.
[20] S. Hayami, Y. Maeda, Inorg. Chim. Acta 255 (1997) 181.
[21] S. Hayami, Z.Z. Gu, M. Shiro, Y. Einaga, A. Fujishima, O. Sato, J. Am. Chem. Soc. 122 (2000) 7126.
[22] G. Juhàsz, S. Hayami, O. Sato, Y. Maeda, Chem. Phys. Lett. 364 (2002) 164.
[23] W.D. Ferder, D.N. Hendrickson, Inorg. Chem. 23 (1984) 3870.
[24] A.J. Conti, R.K. Chadha, K.M. Sena, A.L. Rheingold, D.N. Hendrickson, Inorg. Chem. 32 (1993) 2670.
[25] W.D. Federer, D.N. Hendrickson, Inorg. Chem. 23 (1984) 3861.
[26] (a) M.S. Haddad, W.D. Federer, M.W. Lynch, D.N. Hendrickson, Inorg. Chem. 20 (1981) 123;
(b) M.S. Haddad, W.D. Federer, M.W. Lynch, D.N. Hendrickson, J. Am. Chem. Soc. 102 (1980) 1468;
(c) M.S. Haddad, W.D. Federer, M.W. Lynch, D.N. Hendrickson, Inorg. Chem. 20 (1981) 131.
[27] M.D. Timken, D.N. Hendrickson, E. Sinn, Inorg. Chem. 24 (1985) 3947.
[28] (a) F.V. Wells, S.W. McCann, H.H. Wickman, S.L. Kessel, D.N. Hendrickson, R.D. Feltham, Inorg. Chem. 21 (1982) 2306;
(b) A. Earnshaw, E.A. King, L.F. Larkworthy, J. Chem. Soc. Chem. Commun. (1965) 180;
(c) A. Earnshaw, E.A. King, L.F. Larkworthy, J. Chem. Soc. A (1969) 2459.
[29] K.J. Haller, P.L. Johnson, R.D. Feltham, J.H. Enemark, J.R. Ferraro, L.J. Basile, Inorg. Chim. Acta 33 (1979) 119.
[30] (a) B.W. Fitzsimmons, L.F. Larkworthy, K.A. Rogers, Inorg. Chim. Acta 44 (1980) L53;
(b) E. König, G. Ritter, J. Waigel, L.F. Larkworthy, R.M. Thompson, Inorg. Chem. 26 (1987) 1563.
[31] A.M. Milne, E.N. Maslem, Acta Crystallogr. B44 (1988) 254.
[32] N. Matsumoto, S. Ohta, C. Yoshimura, A. Ohyoshi, S. Kohata, H. Okawa, Y. Maeda, J. Chem. Soc. Dalton. Trans. (1985) 2575.
[33] Y. Maeda, Y. Noda, H. Oshio, Y. Takashima, N. Matsumoto, Hyperfine Interact. 84 (1994) 471.
[34] Y. Nishida, K. Kino, S. Kida, J. Chem. Soc. Dalton Trans. (1987) 1957.
[35] E. Sinn, G. Sim, E.V. Dose, M.F. Tweedle, L.J. Wilson, J. Am. Chem. Soc. 100 (1978) 3375.
[36] Y. Maeda, H. Oshio, Y. Tanigawa, T. Oniki, Y. Takashima, Bull. Chem. Soc. Jpn. 64 (1991) 1522.
[37] (a) J.-P. Costes, F. Dahan, J.-P. Laurent, Inorg. Chem. 29 (1990) 2448;
(b) Y. Maeda, H. Oshio, Y. Takashima, M. Mikuriya, M. Hidaka, Inorg. Chem. 25 (1986) 2958.
[38] (a) Y. Maeda, H. Ohio, K. Toriumi, Y. Takashima, J. Chem. Soc. Dalton Trans. (1991) 1227;
(b) Y. Maeda, N. Tsutsumi, Y. Takashima, Chem. Phys. Lett. 88 (1982) 248.
[39] Y. Maeda, Y. Takashima, N. Matsumoto, A. Ohyoshi, J. Chem. Soc. Dalton Trans. (1986) 1115.
[40] Y. Maeda, H. Oshio, K. Toriumi, Y. Takashima, J. Chem. Soc. Dalton Trans. (1991) 1227.
[41] E.V. Dose, K.M.M. Murphy, L.J. Wilson, J. Chem. Soc. Dalton Trans. (1988) 2927.
[42] M.F. Tweedle, L.J. Wilson, J. Am. Chem. Soc. 98 (1976) 4824.
[43] (a) M. Costas, M.P. Mehn, M.P. Jensen, L. Que Jr., Chem. Rev. 104 (2004) 939;
(b) H.J. Kruger, in: B. Meunier (Ed.), Biomimetic Oxidations, Imperial College Press, London, 2000, p. 363.
[44] (a) A.J. Simaan, M.-L. Boillot, E. Rivière, A. Boussac, J.-J. Girerd, Angew. Chem. Int. Ed. 39 (2000) 196;
(b) A.J. Simaan, M.-L. Boillot, R. Carrasco, J. Cano, J.-J. Girerd, T.A. Mattioli, J. Ensling, H. Spiering, P. Gütlich, Chem. Eur. J. 11 (2005) 1779.
[45] S. Floquet, A.J. Simaan, E. Rivière, M. Nierlilch, P. Thuéry, J. Ensling, P. Gütlich, J.-J. Girerd, M.-L. Boillot, Dalton Trans. (2005) 1734.
[46] M. Nakamura, Coord. Chem. Rev. 250 (2006) 2271.
[47] M.K. Ellison, H. Nasri, Y.-M. Xia, J.-C. Marchon, C.E. Schulz, P.G. Debrunner, W.R. Scheidt, Inorg. Chem. 36 (1997) 4804.

[48] T. Ikeue, Y. Ohgo, T. Yamaguchi, M. Takahashi, M. Takeda, M. Nakamura, Angew. Chem. Int. Ed. 40 (2001) 2617.
[49] Y. Ohgo, Y. Chiba, D. Hashizume, H. Uekusa, T. Ozeki, M. Nakamura, Chem. Commun. (2006) 1935.
[50] R. Boča, Y. Fukuda, M. Gembickỳ, R. Herchel, R. Jaroščiak, W. Linert, F. Renz, J. Yuzuri-hara, Chem. Phys. Lett. 325 (2000) 411.
[51] R. Kitashima, S. Imatomi, M. Yamada, N. Matsumoto, Y. Maeda, Chem. Lett. 34 (2005) 1388.
[52] R. Herchel, R. Boča, M. Gembický, J. Kožíšek, F. Renz, Inorg. Chem. 43 (2004) 4103.
[53] F. Renz, P. Kerep, Hyperfine Interact. 156/157 (2004) 371.
[54] S. Imatomi, R. Kitashima, T. Hamamastu, M. Okeda, Y. Ogawa, B. Matsumoto, Chem. Lett. 5 (2006) 502.
[55] A. Edward, R.L. Martin, E. Sinn, A.H. White, Inorg. Chem. 8 (1969) 1837.
[56] S. Hayami, T. Matoba, S. Nomiyama, T. Kojima, S. Osaki, Y. Maeda, Bull. Chem. Soc. Jpn. 70 (1997) 3001.
[57] R.M. Golding, Mol. Phys. 12 (1967) 13.
[58] J.A. Tjon, M. Blume, Phys. Rev. 165 (1968) 456.
[59] N. Sutin, Acc. Chem. Res. 15 (1982) 275.
[60] A.J. Conti, K. Kaji, Y. Nagano, K.M. Sena, Y. Yumoto, R.K. Chadha, A.L. Rheingold, M. Sorai, D.N. Hendrickson, Inorg. Chem. 32 (1993) 2681.
[61] M. Sorai, Y. Maeda, H. Oshio, J. Phys. Chem. Solids 51 (1990) 941.
[62] (a) R.H. Petty, E.V. Dose, M.F. Tweedle, L.J. Wilson, Inorg. Chem. 17 (1978) 1064;
(b) E.V. Dose, K.M. Murphy, L.J. Wilson, Inorg. Chem. 15 (1976) 2622.
[63] (a) M.S. Hadded, W.D. Federer, M.W. Lynch, D.N. Hendrickson, Inorg. Chem. 20 (1981) 131;
(b) M.S. Hadded, W.D. Federer, M.W. Lynch, D.N. Hendrickson, J. Am. Chem. Soc. 102 (1980) 1468.
[64] A. Hauser, in: P. Gütlich, H.A. Goodwin (Eds.), Spin Crossover in Transition Metal Compounds, vol. II, Springer, Top. Curr. Chem. 234 (2004) 155.
[65] (a) A. Hauser, A. Vef, P. Adler, J. Chem. Phys. 95 (1991) 8710;
(b) A. Vef, U. Manthe, P. Güetlich, A. Hauser, J. Chem. Phys. 101 (1994) 8326.
[66] I. Lawthers, J.J. McGarvey, J. Am. Chem. Soc. 106 (1984) 4280.
[67] S. Hayami, K. Hashiguchi, K. Inoue, Y. Maeda, J. Nucl. Radiochem. Sci. 5 (2004) N1.
[68] S. Hayami, Z.-Z. Gu, H. Yoshiki, A. Fujishima, O. Sato, J. Am. Chem. Soc. 123 (2001) 11644.
[69] S. Floquet, M.-L. Boillot, E. Rivière, F. Varret, K. Boukheddaden, D. Morineau, P. Négrier, New J. Chem. 27 (2003) 341.
[70] C. Enachescu, A. Hauser, J.-J. Girerd, M.-L. Boillot, Chem. Phys. Chem. 7 (2006) 1127.
[71] (a) A. Sour, M.-L. Boillot, R. Rivière, P. Lesot, Eur. J. Inorg. Chem. (1999) 2117;
(b) S. Hirose, S. Hayami, Y. Maeda, Bull. Chem. Soc. Jpn. 73 (2000) 2059.
[72] R. Clément, A. Léaustic, in: J.S. Miller, M. Drillon (Eds.), Magnetism: Molecules to Materials, vol. III, Mol.-Based Mater. (2001) 397.
[73] S. Floquet, S. Salunke, M.-L. Boillot, R. Clément, F. Varret, K. Boukheddaden, E. Rivière, Chem. Mater. 14 (2002) 4164.
[74] S. Mukherjee, T. Weyhermüller, E. Bill, K. Wieghardt, P. Chaudhuri, Inorg. Chem. 44 (2005) 7099.
[75] S. Dorbes, L. Valade, J.A. Real, C. Faulmann, Chem. Commun. (2005) 69.
[76] K. Takahashi, H. Cui, H. Kobayashi, Y. Einaga, O. Sato, Chem. Lett. 34 (2005) 1240.
[77] K. Takahashi, H. Cui, Y. Okano, H. Kobayashi, Y. Einaga, O. Sato, Inorg. Chem. 45 (2006) 5739.